JOURNAL OF BACTERIOLOGY, Mar. 2004, p. 1838–1850 Vol. 186, No. 6
0021-9193/04/$08.00+0 DOI: 10.1128/JB.186.6.1838–1850.2004

Quorum Sensing in *Staphylococcus aureus* Biofilms

Jeremy M. Yarwood,[1] Douglas J. Bartels,[2] Esther M. Volper,[1] and E. Peter Greenberg[1]*

Department of Microbiology, Roy and Lucille Carver College of Medicine, University of Iowa, Iowa City, Iowa 52242,[1] and Vertex Pharmaceuticals, Coralville, Iowa 52240[2]

Received 21 October 2003/Accepted 1 December 2003

Several serious diseases are caused by biofilm-associated *Staphylococcus aureus*, infections in which the accessory gene regulator (*agr*) quorum-sensing system is thought to play an important role. We studied the contribution of *agr* to biofilm development, and we examined *agr*-dependent transcription in biofilms. Under some conditions, disruption of *agr* expression had no discernible influence on biofilm formation, while under others it either inhibited or enhanced biofilm formation. Under those conditions where *agr* expression enhanced biofilm formation, biofilms of an *agr* signaling mutant were particularly sensitive to rifampin but not to oxacillin. Time lapse confocal scanning laser microscopy showed that, similar to the expression of an *agr*-independent fluorescent reporter, biofilm expression of an *agr*-dependent reporter was in patches within cell clusters and oscillated with time. In some cases, loss of fluorescence appeared to coincide with detachment of cells from the biofilm. Our studies indicate that the role of *agr* expression in biofilm development and behavior depends on environmental conditions. We also suggest that detachment of cells expressing *agr* from biofilms may have important clinical implications.

Staphylococcus aureus, a leading cause of nosocomial infections worldwide, is the etiologic agent of a wide range of diseases, from relatively benign skin infections to potentially fatal systemic disorders. Many of these diseases, including endocarditis, osteomyelitis, and foreign-body related infections, appear to be caused by biofilm-associated *S. aureus* (12, 18, 30, and 44). Biofilms are sessile microbial communities embedded in a self-produced extracellular polymeric matrix (12, 44). There is increasing awareness that biofilms have a special clinical relevance. Biofilm-associated bacteria show an innate resistance to antibiotics (5), disinfectants (36), and clearance by host defenses (reference 43; also reviewed in reference 12). These properties likely contribute to the persistence and recalcitrance to treatment of staphylococcal biofilm infections.

Two stages of staphylococcal biofilm formation have been described (reviewed in reference 18). The first stage involves attachment of cells to a surface. This stage of biofilm formation is likely to be mediated in part by cell wall-associated adhesins, including the microbial surface components recognizing adhesive matrix molecules. The second stage of biofilm development includes cell multiplication and formation of a mature structure consisting of many cell layers. This stage is associated with the production of extracellular factors, including the polysaccharide intercellular adhesin component of the extracellular matrix.

Intercellular signaling, often referred to as quorum sensing, has been shown to be involved in biofilm development by several bacteria, including *Pseudomonas aeruginosa* (11), *Burkholderia cepacia* (22, 23), *Streptococcus mutans* (26, 31), and others (27, 46, 49). For example, a quorum-sensing-defective mutant of *P. aeruginosa* is unable to form the highly differentiated biofilm structure associated with wild-type *P. aeruginosa*, at least under certain conditions (11). *S. aureus* quorum sensing involves a system unrelated to the *P. aeruginosa* acyl-homoserine lactone system. The *S. aureus* quorum-sensing system is encoded by the accessory gene regulator (*agr*) locus (reviewed in references 35 and 39). The *agr* system contributes to virulence in model biofilm-associated infections, including endocarditis (7, 50) and osteomyelitis (3, 15), although the precise role of the *agr* system varies with the type of infection model used (16, 17, 54). The *agr* locus consists of two divergent operons driven by the P2 and P3 promoters. The P2 operon contains *agrBDCA* and codes for the RNAII transcript. P3 drives transcription of RNAIII, the effector molecule of the *agr* locus. Also, δ-hemolysin, a secreted virulence factor encoded by *hld*, is translated from RNAIII. AgrA and AgrC comprise a two-component regulatory system that responds to the secreted autoinducing cyclic octapeptide. The autoinducing cyclic octapeptide is processed from the *agrD* product by AgrB. Signaling via this system, in concert with other regulatory elements, such as SarA (6), increases transcription from both the P2 and P3 promoters, resulting in elevated intracellular concentrations of RNAIII. In batch culture, RNAIII acts to increase the expression of secreted virulence factors and decrease the expression of several surface adhesins, including protein A and the fibronectin-binding protein.

Some information about the relationship between *agr* expression and *S. aureus* biofilms is available. Pratten et al. (38) found little difference between wild-type *S. aureus* and an *agr* mutant in adherence to either uncoated or fibronectin-coated glass under flow conditions. Furthermore, expression of *hld* was highest near the base of the biofilm, where the highest numbers of bacteria was also observed. Shenkman et al. (42) found that RNAIII expression decreased *S. aureus* adherence to fibrinogen under static conditions and increased adherence

* Corresponding author. Mailing address: 540 EMRB, Department of Microbiology, Roy and Lucille Carver College of Medicine, University of Iowa, Iowa City, IA 52242. Phone: (319) 335-7775. Fax: (319) 335-7949. E-mail: everett-greenberg@uiowa.edu.

to fibronectin and human endothelial cells under both static and flow conditions. Vuong et al. (51) examined the correlation between a functional *agr* system and the ability of *S. aureus* clinical isolates to adhere to polystyrene under static conditions. Only 6% of the isolates with a functional *agr* system formed a biofilm under these conditions compared to 78% of the *agr*-defective isolates. The failure of the strains with functional *agr* loci to form a biofilm was thought to be due in part to the surfactant properties of δ-hemolysin. Another exotoxin directly regulated by the *agr* system, alpha-toxin, was recently found to contribute to biofilm formation under both static and flow conditions (4). In an experimental endocarditis study, RNAIII activation was time and cell density dependent and occurred through both RNAII-dependent and -independent mechanisms (53). Taken together, these studies indicate that the precise role of *agr* expression in biofilm development is dependent upon the conditions under which the biofilm is grown. However, the studies were done using different strains, and it remains to be determined whether the differing results were a consequence of different conditions or different strains.

Several questions regarding the role of *agr* expression in biofilm behavior and function, particularly in the second stage of biofilm formation, remain to be addressed. Can quorum sensing affect the structure and development of *S. aureus* biofilms? Can the contribution of the *agr* system to biofilm development change when biofilms of the same strain are grown under different conditions? Does quorum sensing affect the antibiotic resistance of *S. aureus* biofilms? When and where are *agr*-controlled transcripts activated in biofilms, and might this have implications for the pathogenesis of biofilm-associated infections? To begin to address these questions, we have examined the effects of *agr* expression on biofilm development and antibiotic resistance under both static and flow conditions. We have also employed time lapse confocal scanning laser microscopy (CSLM) and green fluorescent protein (GFP) technology to examine *agr*-dependent expression in biofilms.

MATERIALS AND METHODS

Bacterial strains, plasmids, and culture conditions. The strains and plasmids used are described in Table 1. Planktonic cultures of either *S. aureus* or *Escherichia coli* DHα were grown in Luria-Bertani (LB) broth or plated on LB agar with the appropriate antibiotics for plasmid selection or maintenance (erythromycin, 5 μg/ml; chloramphenicol, 10 μg/ml; ampicillin, 100 μg/ml) and incubated at 37°C. The medium for growth of static biofilms in microtiter dishes was Bacto Tryptic Soy Broth (TSB) (Becton Dickinson, Sparks, Md.) plus 1% glucose and 2% NaCl. We used 5% TSB as the growth medium for the spinning-disk biofilms. For most flow cell experiments, we used a medium containing 2% LB broth and 0.1% glucose. Where indicated, we used 5% TSB in flow cell experiments. When required, 5 μg of erythromycin/ml was added to the flow cell media to maintain reporter plasmids. All biofilm cultures were incubated at 37°C unless otherwise indicated.

Strain and plasmid construction. The PCR primers used are listed in Table 1. Generally, we used *E. coli* throughout plasmid construction. The plasmids were then used to transform *S. aureus* RN4220, and RN4220-modified plasmids were used to transform *S. aureus* MN8. In all cases, *S. aureus* was transformed by electroporation (40).

To construct the *agrD* mutant, *S. aureus* MN8 was transformed with the temperature-sensitive plasmid pDB60, which contains an *ermC* erythromycin resistance cassette flanked by a 2,219-bp *agrAC*-containing fragment and a 2,349-bp *agrB* P3-containing fragment. Transformants were grown at 42°C, and a chloramphenicol-sensitive, erythromycin-resistant transformant was selected for further study. A chromosomal deletion of the *agrD* region was confirmed by Southern analysis, and the mutant produced only 20% of the parental levels of toxic shock syndrome toxin 1 as measured by an enzyme-linked immunosorbent assay (14, 55). Furthermore, unlike the parent, the *agrD* mutant containing an *agr*-dependent *gfp* expression vector showed background fluorescence in planktonic or biofilm cultures (data not shown). The sequence data for the design of primers to amplify portions of the *agr* locus for pDB60 were obtained from the *S. aureus* MRSA252 Sequencing Group at the Sanger Institute (ftp://ftp.sanger.ac.uk/pub/pathogens/sa).

The reporter plasmid pDB22 contains a fusion of the *agr* P3 promoter region (bp 508 to 605; GenBank accession number AF288215) with gfp_{mut2} (a gene coding for a bright variant of GFP). The P3 promoter fragment extends 53 bp upstream of the −35 region and is sufficient for *agr*-dependent transcription of RNAIII as described by Morfeldt et al. (32). The reporter plasmid pJY202 contains a fusion of nearly the entire *agr* P2-P3 intergenic region (bp 490 to 711; GenBank accession number AF288215) with yfp_{10B} (a gene coding for a different bright variant of GFP). The yfp_{10B} gene contained a T7 *gene10* Shine-Delgarno sequence created as follows. The *gene10* Shine-Delgarno sequence from pKEN was PCR amplified using primers O93 and O94. This PCR product was then used as a primer in a second PCR, together with primers O93 and O97 and pRSET-10B as a template, to amplify *yfp*10B. The fragment was cloned into a pUC18-pC194 shuttle vector to form pDB39. The reporter plasmid pJY209 contains a fusion of 257 bp of the *sar* P1 promoter (bp 601 to 857; GenBank accession number U46541) (8, 29) with yfp_{10B}.

Fluorescence levels for each of these reporters were determined using flow cytometry (FACScan; Becton Dickinson). Appropriate settings for flow cytometry were determined by analyzing known mixtures of GFP-fluorescent and nonfluorescent *S. aureus* cells using the FL-1 channel. Ten thousand cells from stationary-phase cultures of each strain were then analyzed using identical flow cytometry settings, and the data were analyzed using CellQuest (version 3.1f) software. The average fluorescence of the strain with the *agr* P3 reporter plasmid pDB22 was 11 times that of the parental strain (MN8) with no reporter and ~4 times the minimum fluorescence required for visualization by confocal microscopy. The average fluorescence of the strain with the *agr* P3 reporter plasmid pJY202 was 163 times that of parental cells and ~60 times the minimum fluorescence required for visualization by confocal microscopy. The average fluorescence of the strain with the *sar* P1 reporter plasmid pJY209 was 40 times that of parental cells and 14 times the minimum fluorescence required for visualization by confocal microscopy. The plasmid copy number for pE194-based plasmids during growth of *S. aureus* at 32°C is estimated to be 10 to 25 per cell; growth at 37°C is thought to reduce the copy number (52).

Biofilm experiments. We used three different biofilm growth systems, a static microtiter dish system, a rotating-disk reactor system, and a flow cell system. The static biofilm system was similar to that described by Christensen et al. (9). The medium described above was inoculated with overnight *S. aureus* cultures (1% [vol/vol]). The inoculated medium was dispensed into wells of sterile flat-bottom 96-well polystyrene tissue culture plates (Costar no. 3596; Corning Inc., Corning, N.Y.) at 0.2 ml per well. The plates were incubated for 18 h without shaking. The liquid in the wells was removed by aspiration, and the wells were washed once with 0.2 ml of sterile phosphate-buffered saline (PBS). Bacteria attached to the plastic were fixed with Bouin fixative and stained with 1% crystal violet. Excess stain was removed by washing the plates with distilled water. The crystal violet absorbance at 595 nm was measured by using a Tecan GENios microtiter dish reader (Phenix Research Products, Research Triangle Park, N.C.).

The rotating-disk reactor was similar to that described previously (20) with some modification. The reactor was inoculated with an overnight culture of *S. aureus* (1% [vol/vol]), and after overnight growth a flow of fresh medium was initiated (dilution rate, 0.7 h^{-1}). After an additional 24-h incubation, polycarbonate chips with attached biofilm bacteria were removed from the spinning disk and washed three times in PBS. The remaining attached cells were dispersed into 2 ml of PBS by using a tissue homogenizer (Brinkman). Total CFU were determined by dilution and plating on LB agar.

We used a flow cell bioreactor for studies of gene expression and biofilm development (37). The flow cells were inoculated with stationary-phase cultures, and flow was initiated after a 1-h incubation at room temperature. The flow rate was laminar, with a Reynolds number of 0.17. To ensure that functional reporter plasmids were maintained during biofilm growth, we recovered bacteria by using high fluid shear to expel biofilms from flow cells with PBS and plating the material on LB agar with and without antibiotics. When *S. aureus* containing erythromycin-resistant reporters was removed from 6-day-old biofilms, equal numbers of colonies arose on LB agar and on LB agar with erythromycin.

The numbers of fluorescent cells in flow cell biofilms and from flow cell effluents were measured by flow cytometry. Effluent from the flow cells was collected for ~30 min, and then the biofilms were expelled from the flow cells by the high shear force of 12 ml of fresh growth medium forced through the system by using a syringe. This expulsion of biofilm left only a thin layer of nonfluores-

TABLE 1. Strains, plasmids and primers used in this study

Strain, plasmid, or primer	Relevant characteristics	Source or reference
S. aureus		
RN4220	$r_K^- m_K^+$	24
MN8	*tstH*$^+$; clinical isolate from nonmenstrual toxic shock syndrome case	41
AMD283	MN8 *agrD*	This study
Plasmids		
LITMUS28	Cloning vector	New England Biolabs
pCR2.1-TOPO	TA cloning vector	Invitrogen
pKEN-GFPmut2	gfp_{mut2}	10
pRSET10-B	yfp_{10B}	R. Heim
pE194	*ermC*	19
pCE104	Shuttle vector containing pE194 and pUC18; Em^r	33
pCE107	pCE104 containing *Hin*dIII-*Sal*I MN8 *tstH* chromosomal fragment; Em^r	P. Schlievert
pKSV7	pUC18-pC194 chimera; temperature sensitive; Cm^r	45
pDB1	PCR-amplified (O1 and O2) *agr* region from RN4220 cloned into *Xho*I-*Hin*dIII-digested LITMUS28	This study
pDB2	*Bam*HI-*Pst*I gfp_{mut2} from pKEN cloned into *Bam*HI-*Pst*I-digested LITMUS28	This study
pDB3	PCR-amplified *ermC* from pE194 cloned into *Eco*RI- and *Bgl*II-digested LITMUS28	This study
pDB4	*Bgl*II*Eco*RI *ermC* fragment from pDB3 cloned into *Bgl*II- and *Eco*RI-digested pDB2	This study
pDB6	pUC18 containing *XhoI* (*Sal*I)-*Hin*dIII *agr* fragment from pDB1	This study
pDB9	pDB6 with *Bgl*II site introduced into the RNAIII region using O35, O36	This study
pDB12	*Bam*HI-*Bgl*II gfp_{mut2} *ermC* fragment from pDB4 cloned into *Bgl*II-digested pDB9	This study
pDB13	*Bam*HI-*Hin*dIII *agr* P3-gfp_{mut2} *ermC* fragment from pDB12 cloned into *Bam*HI- and *Hin*dIII-digested pCE107	This study
pDB22	*agr* P3-gfp_{mut2} reporter; PCR-amplified (O1 and O62) *agr* P3-gfp_{mut2} *ermC* fragment from pDB13 cloned into *Bam*HI-*Hin*dIII-digested pCE107	This study
pDB39	pUC18/pC194 shuttle vector containing *Bam*HI-*Bgl*II yfp_{10B} fragment from pDB44	This study
pDB44	pCR2.1-TOPO containing yfp_{10B} PCR amplified from *Bam*HI-digested pRSET10-B, yfp_{10B} contains *gene10* ribosome-binding site	This study
pDB52	*Bam*HI-*Bgl*II fragment (containing *ermC*) of pDB3 cloned into *Bam*HI-digested pKSV7	This study
pDB53	*agrCA* fragment PCR amplified from MN8 (O63 and O68) and cloned into *Xba*I-digested pDB52	This study
pDB59	PCR-amplified (O110 and O111) *agr* P2-P3 region from MN8 cloned into *Bam*HI-digested pDB39; *agr* P3-yfp_{10B}; Cm^r	This study
pDB60	*agrB*-P3 fragment PCR amplified (O112 and O113) from MN8 and cloned into *Bam*HI- and *Bgl*II-digested pDB53	This study
pDB63	PCR-amplified (O126 and O127) *sar* P1 region from MN8 cloned into *Bam*HI-digested pDB39; Cm^r	This study
pJY202	*agr* P3-yfp_{10B} reporter; pCE104 containing *agr* P3-yfp_{10B} *Kpn*I-*Hin*dIII fragment of pDB59; Em^r	This study
pJY209	*sar* P1-yfp_{10B} reporter; pCE104 containing *sar* P1-yfp_{10B} *Kpn*I-*Hin*dIII fragment of pDB63; Em^r	This study
Primer (5′-3′)		
O1	TATATAAGCTTGAGCTTGGGAGGGGCTCACGACC	
O2	TATATCTCGAGAGCTTGCTCAAGCACCTCATAAGG	
O20	ATGATCGAATTCTTATTTGTACAATTCA	
O35	GCTTTTAGCATGTTTTAATATAACTAGATCTCAGAGATGTGATGGAAAATAG	
O36	CTATTTTCCATCACATCTCTGAGATCTAGTTATATTAAAACATGCTAAAAGC	
O62	ATAATGGATCCATTTTAACATAAAAAAATTTACAGTTAAG	
O63	GCACGTCTAGAGGTATACAATGAAACGTTGTATCG	
O68	ATACTCTCTAGACTATAAGAGAAAGTGTGATAG	
O93	ATGGGAAGCTTCGTGGATCCTCTAGATTTAAG	
O94	GTTCTTCTCCTTTACTCATATGTATATCTCC	
O97	CGCTGGCAGATCTTTATTATTTGTATAGTTCATCCATGCC	
O110	GGATCCACCACTCTCCTCACTGTTATTATACGA	
O111	AGATCTTTTTCCATCACATCTCTGTGATCTAGT	
O112	TAGATCTATCAAGGATGTGATGTTATGAAAGT	
O113	AGGATCCTTTTTCATAATTTAGTCCTCCTTTGAA	
O126	GGATCCGCTGATATTTTTGACTAAACCAAATG	
O127	GAGATCTCCTCCCTATTTGATGCATCTTG	

cent cells attached to the glass surface. Both the biofilm-derived cells and cells in the biofilm effluents were dispersed by sonication (Branson Sonifier 250) at 40% power for ~5 s. This treatment did not affect cell numbers or fluorescence in stationary-phase batch cultures of a strain carrying the *agr* P3-*gfp* reporter (pJY202). Five thousand biofilm-derived cells from each sample were analyzed for green fluorescence as described above.

Where indicated, flow cell biofilms were stained with either of two nucleic acid stains, SYTO62 (Molecular Probes, Eugene, Oreg.) or propidium iodide (Sigma

Chemical Co., St. Louis, Mo.). SYTO62 penetrates and stains nucleic acids in both live and dead cells. Because SYTO62 reduces cell viability, we used it only at experimental endpoints. Propidium iodide is thought to be unable to penetrate viable cells and was thus maintained at 4 μM in the flow cell medium reservoir to allow visualization of the overall biofilm structure by time lapse CSLM. The addition of 4 μM propidium iodide to batch cultures did not affect the growth of *S. aureus* (pDB22), nor did it affect the detection of GFP fluorescence.

Antibiotic resistance. Standardized planktonic antibiotic MICs were determined using the broth microdilution method as described by the NCCLS (34). We assessed the resistance of biofilm cells to antibiotics as follows. Biofilms grown in the rotating-disk reactor were washed as described above and incubated in 1 ml of LB broth with antibiotics for 5 h in 24-well tissue culture plate wells (Falcon no. 353047; Becton Dickinson Labware, Franklin Lakes, N.J.). The numbers of viable cells remaining were determined by homogenization and plating as described above.

Microscopy. For CSLM, we used a Radiance 2100 system (Bio-Rad, Hercules, Calif.) with a Nikon Eclipse E600 microscope contained in a microscope temperature control system (Life Imaging Services, Reinach, Switzerland). The excitation wavelength used for GFP was 488 nm (argon laser), and the emission was collected at 515 ± 15 nm. To detect propidium iodide fluorescence, excitation was at 488 nm and emission wavelengths of >660 nm were collected with a 660LP filter. To detect the red fluorescent nucleic acid stain SYTO62, excitation was at 637 nm and emission wavelengths of >660 nm were collected. For the time course experiments, flow cells were incubated on the microscope stage at 37°C and *z*-series images were acquired at 15-min intervals. The biofilms were exposed to the scanning laser for ~45 s at each interval. The image acquisition software was LaserSharp 2000 (Bio-Rad). Postacquisition, images were processed using Confocal Assistant or Volocity (Improvision, Lexington, Mass.) software. Nikon 20× (Plan Fluor) and 60× (Plan Apo) objective lenses were used for CSLM. For phase-contrast microscopy of flow cell biofilms, we used an Olympus BX-51 microscope with a 20× objective lens.

Fluorescence detection in batch cultures. GFP fluorescence in batch cultures of *S. aureus* containing either pDB22 or pJY202 was measured in a Tecan microtiter dish reader with an excitation wavelength of 485 nm and an emission wavelength of 535 nm. Relative fluorescence units were determined by subtracting the background fluorescence (*S. aureus* without a GFP plasmid) from the absolute fluorescence.

RESULTS

The *agr* system in *S. aureus* biofilm development and antibiotic resistance. We first tested the ability of an *agrD* deletion mutant (AMD 283) and its parent (MN8) to form biofilms in a static biofilm system. Consistent with a previous study comparing quorum-sensing-competent and quorum-sensing-defective clinical isolates under static conditions (51), the *agrD* mutant formed larger biofilms than did the parent strain (Fig. 1A). We were interested in several additional questions. What is the influence of quorum sensing on the development of biofilms subjected to shear forces introduced by flow? Does quorum sensing influence antibiotic resistance in biofilms? When are quorum-induced genes expressed in the biofilm? To address these questions, we used two separate systems in which there was a continuous flow of medium. One system, a once flowthrough apparatus, allows direct microscope observation of biofilms generated under relatively low shear forces. The other system, a rotating-disk reactor, allows one to easily remove biofilms for further study but is not suited for analyzing the structure of a growing biofilm. The shear forces in a rotating-disk reactor are much higher than in a flow cell; the velocity of the medium over the biofilm surface is ~1,500-fold higher in the rotating-disk reactor than in the flow cell.

When we used a rotating-disk reactor, the parent biofilms contained 10-fold more CFU per chip than did the *agrD* mutant (Fig. 1B). Microscopy showed few, if any, *S. aureus* cells remaining on the chips after homogenization. Furthermore, cells released from the both the parent and *agrD* mutant biofilms by homogenization were either individuals or pairs but not clusters.

We detected no significant differences in the structures or thicknesses of the biofilms formed in flow cells by the *agrD* deletion mutant and its parent over a period of 5 days (Fig. 1C). The biofilms were viewed once a day using both phase-contrast microscopy and CSLM, and representative CSLM images are shown in Fig. 1C. For both strains, biofilms covered the majority of the glass surface within 48 h, and large clusters of cells that protruded from the glass surface (microcolonies) developed and persisted for the remainder of the experiment. The images shown are from an experiment in which we used 2% LB broth plus 0.1% glucose as the growth medium. In flow cell experiments with 5% TSB, biofilms developed more rapidly, but we still could not detect any differences between the parent and *agrD* mutant biofilms. Taken together, the results from the three different systems indicate that the contribution of the *agr* system to biofilm development is dependent upon the biofilm growth conditions.

We exposed biofilms of wild-type *S. aureus* and the *agrD* mutant grown in the rotating-disk reactor to two clinically relevant antibiotics, rifampin and oxacillin. Biofilms of the parent strain, MN8, showed appreciable resistance to both antibiotics (Fig. 2). Even at the highest concentrations tested, 100 μg/ml (50 to 100 times the MIC for planktonic cells), the level of killing was <2 log units. The sensitivity of the *agrD* mutant to oxacillin was similar to that of the parent, but the *agrD* mutant was much more sensitive to rifampin than was the parent. In planktonic cultures, the MICs of rifampin and oxacillin were 0.016 and 0.16 μg/ml, respectively, for both the parent and the mutant strains. These are consistent with the published MICs of rifampin and oxacillin against sensitive *S. aureus* (28). Thus, at least under some conditions, *agr* expression is involved in biofilm resistance to certain antibiotics. This may have some clinical relevance, as rifampin is often used together with other antibiotics in cases of biofilm-associated staphylococcal infections.

Expression of *agr* P3-*gfp* reporters in *S. aureus* biofilms. Though *agr* did not appear to have a significant effect on flow cell biofilm structure, we wondered whether it was expressed in this system and might still have an impact on staphylococcal biofilm biology. To visualize patterns of quorum-sensing-dependent gene expression in *S. aureus* flow cell biofilms, we constructed two reporter plasmids and introduced them into *S. aureus* MN8. These contained either the minimum P3 promoter region required for *agr*-dependent expression of RNAIII (32) fused to a *gfp* variant (pDB22) or a fragment extending farther upstream of the P3 promoter fused to a second *gfp* variant (pJY202). In broth culture, *S. aureus* MN8 containing pDB22 or pJY202 exhibited increasing fluorescence beginning in late exponential growth and continuing into stationary phase, as expected of an *agr*-dependent reporter. Most cells in stationary-phase cultures exhibited fluorescence. Furthermore, the *agr* P3-*gfp* plasmids were maintained in viable cells during biofilm growth in flow cells, as indicated by plating in the presence or absence of erythromycin. Thus, these constructs seemed well suited for studies of *agr*-dependent gene expression in biofilm cells.

We followed expression of the *agr* P3-*gfp* reporters in flow

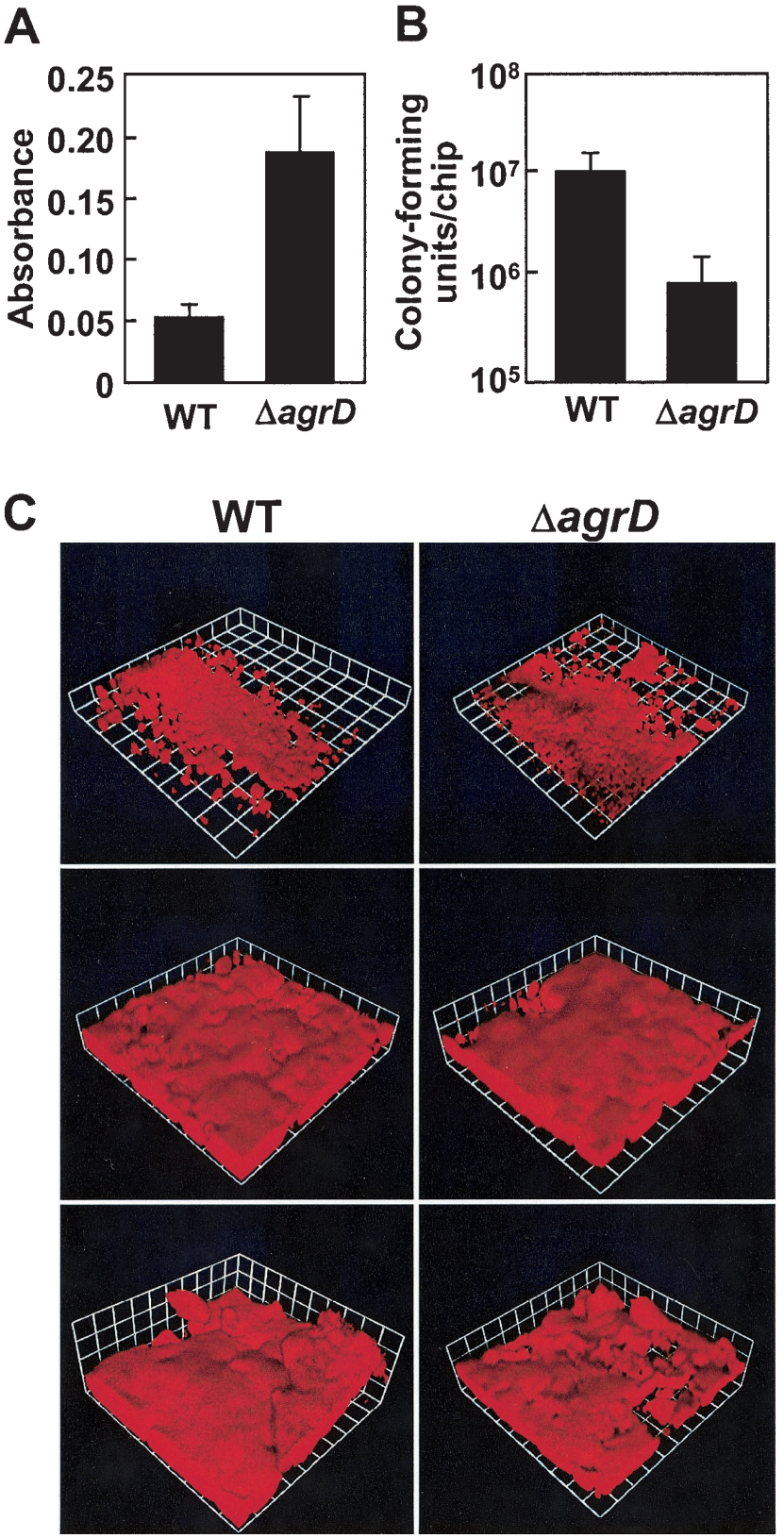

FIG. 1. Influence of *agr* on biofilm development under different growth conditions. The *S. aureus* parent strain, MN8 (WT), and the *agrD* mutant (Δ*agrD*) were grown in microtiter dish assays (A), spinning-disk reactors (B), and flow cells (C). (A) Microtiter dish biofilm mass as measured by crystal violet staining. The data represent the means and standard deviations of 18 replicate wells. (B) CFU recovered from rotating-disk reactor chips. The data represent the means and standard deviations of duplicate chips taken from each of four independent

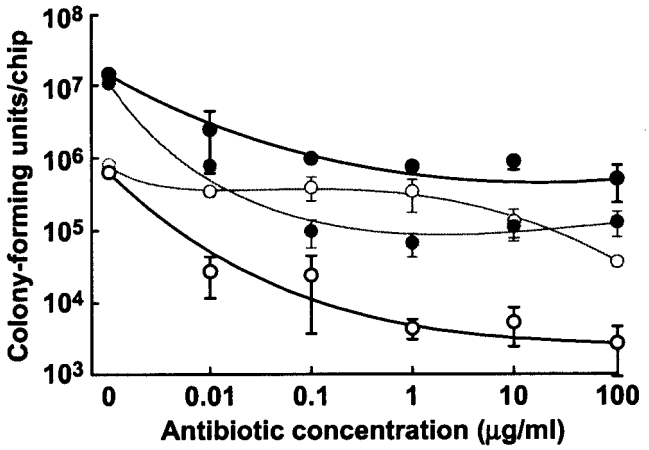

FIG. 2. Quorum sensing and biofilm resistance to antibiotics. Spinning-disk reactor biofilms of the *S. aureus* parent strain, MN8 (solid circles), or the *agrD* mutant AMD283 (open circles) were treated with rifampin (bold lines) or oxacillin (thin lines), and survival was determined by plate counts. The data are averages from two chips from each of two spinning-disk bioreactors for each strain ± the range of means.

cell biofilms by CSLM. GFP was expressed in some, but not all, biofilm cells, as exemplified by the images of a 24-h biofilm of *S. aureus* MN8 (pDB22) (Fig. 3). Clusters of cells could be seen on the glass surface, some of which contained patches of cells expressing the reporter. Not all cells in a cluster expressed *gfp*, and some clusters contained few, if any, cells expressing *gfp*.

To gain insights into the complicated pattern of *agr* P3-*gfp* expression in biofilms, we followed the fluorescence of *S. aureus* MN8(pDB22) by using time lapse confocal microscopy. Images were acquired every 15 min over a 40-h period, and Fig. 4 shows images at 90-min intervals (the complete time lapse series can be viewed as a movie at http://www.medicine.uiowa.edu/greenberglab/Staphylococcus_aureus.htm). Inoculum cells initially exhibited fluorescence, but this fluorescence was lost by 3 h postinoculation. Fluorescent cells then began to appear 4 h after inoculation of the flow cell. There was an oscillation in *gfp* expression which appeared as three waves, periods in which local fluorescence increased and decreased. The first wave of fluorescence lasted ~16 h (4 to 20 h postinoculation), with peak fluorescence at 10 h. The second wave included 20 to 31 h postinoculation, with peak fluorescence at 23 to 24 h. The third wave of fluorescence spanned the period from 32 to 40 h postinoculation, with peak fluorescence at ~35 h. Within the span of a wave, the fluorescence peaked at different times in different areas of the region under observation. Finally, the fluorescence was progressively less intense with each wave. Despite the loss of fluorescence, most of the region under observation was covered by the biofilm (average biofilm depth, ~30 μm), as shown by staining with SYTO62 (Fig. 4, final image). Other flow cell biofilms of *S. aureus* MN8(pDB22) incubated for longer periods showed only sparse fluorescence after 3 days.

During the time lapse experiment, fluorescence declined rapidly after reaching its peak within a given area of the biofilm. In some cases, brightly fluorescent cells could be observed in one image and not in the image acquired 15 min later. This loss of fluorescence was sometimes followed by the appearance of fluorescent cells in the same area of the biofilm, as exemplified by the central microcolony in Fig. 4 (7 to 17.5 h). These observations suggest that the loss of fluorescence might result from the detachment of cells from the biofilm rather than degradation of GFP, which is normally a stable protein in eubacteria (1, 47).

To examine the disappearance of fluorescent cells more closely, we grew a biofilm of *S. aureus* MN8(pJY202) in the presence of propidium iodide so that the biofilm structure and reporter expression could be imaged simultaneously (Fig. 5 and http://www.medicine.uiowa.edu/greenberglab/Staphylococcus_aureus.htm). There was a rapid loss of GFP fluorescence, usually through the entire depth of the biofilm, beginning from the centers of fluorescent clusters and progressing toward the outsides of these clusters (Fig. 5A). The loss of GFP fluorescence appeared to leave large unstained areas within the biofilm. Subsequently, fluorescence returned from the outer edges of these unstained areas toward the center. The unstained areas eventually became filled with cells expressing GFP, as well as stained biofilm matrix. This suggests that the original fluorescent cells had detached from the biofilm, leaving a void behind which was subsequently occupied as a result of new growth. We also observed that some cells along the peripheries of the microcolonies were originally green fluorescent, subsequently lost green fluorescence, and then appeared to stain with propidium iodide, suggesting that the cells were no longer viable. This disappearance and reappearance of GFP fluorescence appeared to occur simultaneously across the entire span of the nearly 500-μm-diameter microcolony in Fig. 5. A three-dimensional reconstruction of the biofilm at a single time point (Fig. 5B) shows fluorescence occurring in valleys within the biofilm, consistent with the loss of cells previously occupying those areas. This active detachment of cells expressing GFP from the biofilm should result in effluents from flow cells that contain a higher percentage of green fluorescent cells than the flow cell biofilm itself. We confirmed that this was the case using flow cytometry (Fig. 6).

To determine whether the pattern of expression observed was unique to *agr* P3-*gfp* reporters, we also examined the expression over time of a *sar* P1-*gfp* reporter fusion. SarA has been shown to be necessary for biofilm formation (2, 48). *sar*

spinning-disk reactors (total, eight chips) for each strain. There is a significant difference between the two strains ($P = 0.03$; Student's t test). (C) Three-dimensional reconstructions from days 1 (top) and 5 (middle and bottom) in flow cell biofilms stained with propidium iodide. Each side of a grid square is 60 μm. Microcolony sizes of biofilms of the wild type and the *agrD* mutant at 48 h were not significantly different. The average surface areas covered by microcolonies in biofilms of the parent and mutant were 0.020 and 0.025 mm^2, respectively (determined by measuring 14 microcolonies of each strain in four different images acquired by light microscopy from two independent flow cell experiments; $P = 0.43$; Student's t test).

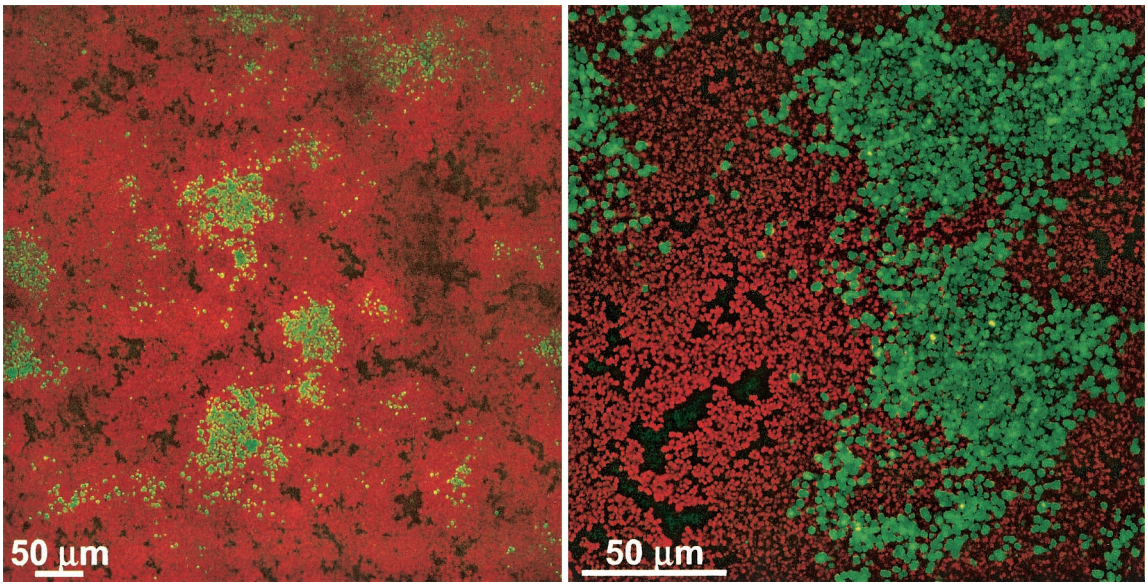

FIG. 3. Expression of the *agr* P3-*gfp* reporter in flow cell biofilms of *S. aureus* MN8(pDB22). The images were acquired by CSLM with either a 20× (left) or 60× (right) objective lens. The images represent a compressed *z* series, where multiple *x-y* planes from top to bottom of the biofilm are combined. Green indicates those cells expressing GFP; all other cells appear red from treatment with SYTO62.

P1-*gfp* reporters were expressed throughout growth in vitro (mid-log, late log, and stationary phases), were expressed in vivo throughout an endocarditis vegetation (8, 29), and have been used as de facto constitutive reporters to visualize staphylococcal biofilms (25). Similarly, expression of our reporter was detected throughout the growth of the organism in vitro, and its expression was not altered by mutation of *agrD*. Thus, it seemed suitable for use a reporter to which we could compare *agr* P3-*gfp* expression. Fluorescence from expression of the *sar* P1-*gfp* reporter was initially detected in all visible cells in the biofilm, even within very small microcolonies, suggesting that the *sar* P1 reporter was expressed constitutively. We observed disappearance and reappearance of fluorescence similar to that observed using the *agr* P3 reporter (Fig. 7 and www.medicine.uiowa.edu/greenberglab/Staphylococcus_aureus.htm). This was also demonstrated using a *sar* P1-*gfp* reporter kindly provided by A. Cheung (data not shown). This suggested that the expression patterns observed were not unique to *agr* P3-controlled reporters.

DISCUSSION

We have addressed two basic questions about quorum sensing in *S. aureus* biofilms: what is the influence of the *agr* quorum-sensing system on *S. aureus* biofilm development and antibiotic resistance and what is the pattern of *agr*-dependent gene expression in an *S. aureus* biofilm? With regard to the first question, we used isogenic strains to show that the influence of the *agr* system on biofilm development depends on the conditions of the experiment. Under some conditions, *agr* expression appears to enhance biofilm development; under other conditions, it has no discernible affect or seems to impair biofilm development (Fig. 1). Our experiments help unify what may have been considered disparate conclusions in the literature, and they extend our understanding by showing that the different results reported elsewhere do not necessarily result from strain differences.

We show that under at least one experimental condition *agr* expression can influence a clinically relevant aspect of biofilm biology, antibiotic resistance (Fig. 2). Spinning-disk reactor biofilm cells of our *agrD* mutant were particularly sensitive to rifampin but not to oxacillin. We do not understand the basis of the enhanced biofilm sensitivity to rifampin in the quorum-sensing mutant. This is not a general effect of *agr* expression on rifampin resistance, because nonbiofilm cells of the mutant did not appear to be more sensitive to rifampin than the parent. The antibiotic resistance experiment was done under conditions where the *agr* mutant biofilm contained fewer cells than the parent biofilm. Thus, there may be a rifampin-specific biofilm inoculum effect. Regardless, it is clear that *agr* expression can have important and specific effects on cells in *S. aureus* biofilms. Because rifampin is often used in the treatment of *S. aureus* biofilm infections, further investigation of the influence of *agr* expression on biofilm sensitivity to antibiotics is warranted.

Previous reports have implicated acyl-HSL quorum sensing in the biofilm development of several species of proteobacteria under certain conditions (11, 22, 23, 27, 31, 46). For example, *P. aeruginosa* biofilm development into mushroom-shaped structures has been reported to be dependent on acyl-HSL signaling (11). Under conditions where biofilms do not develop mushroom-like structures, acyl-HSLs do not appear to influence biofilm structure (21). A similar situation may occur with *agr*-dependent quorum sensing in *S. aureus*. Under certain conditions, quorum sensing can play a role in biofilm development, but it may not have an obvious role in biofilm development under all conditions. As the *agr* system is thought to exert regulatory control over a

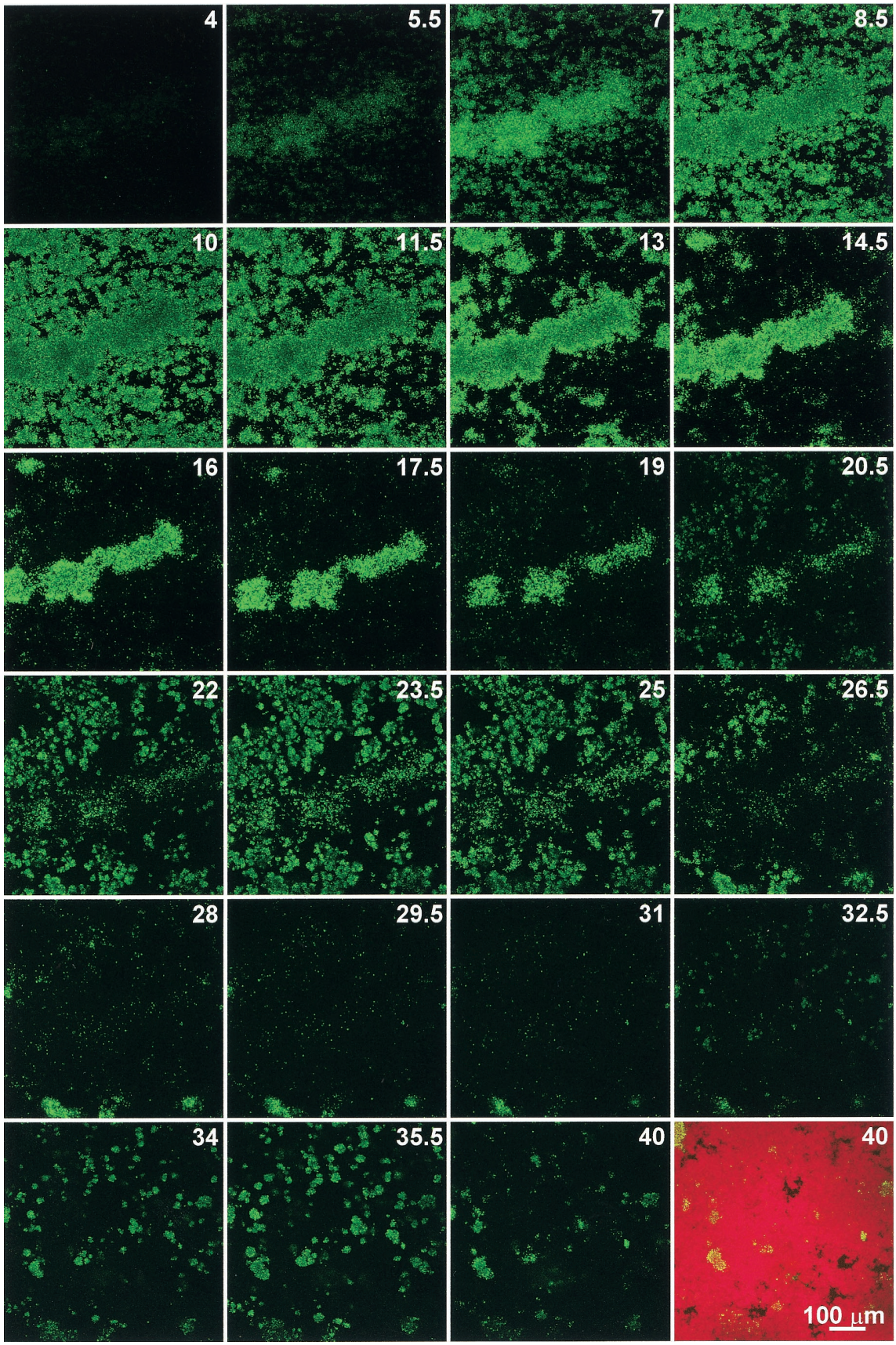

FIG. 4. Time lapse expression of the *agr* P3-*gfp* reporter in a flow cell biofilm of *S. aureus* MN8(pDB22). The images were acquired at 15-min intervals by using identical CSLM settings with a 20× objective lens. Sequential images taken every 90 min are shown, with the number of hours postinoculation indicated. The final image (40 h postinoculation) is shown before and after treatment with SYTO62. The images represent a compressed *z* series, where multiple *x-y* planes from top to bottom of the biofilm are combined.

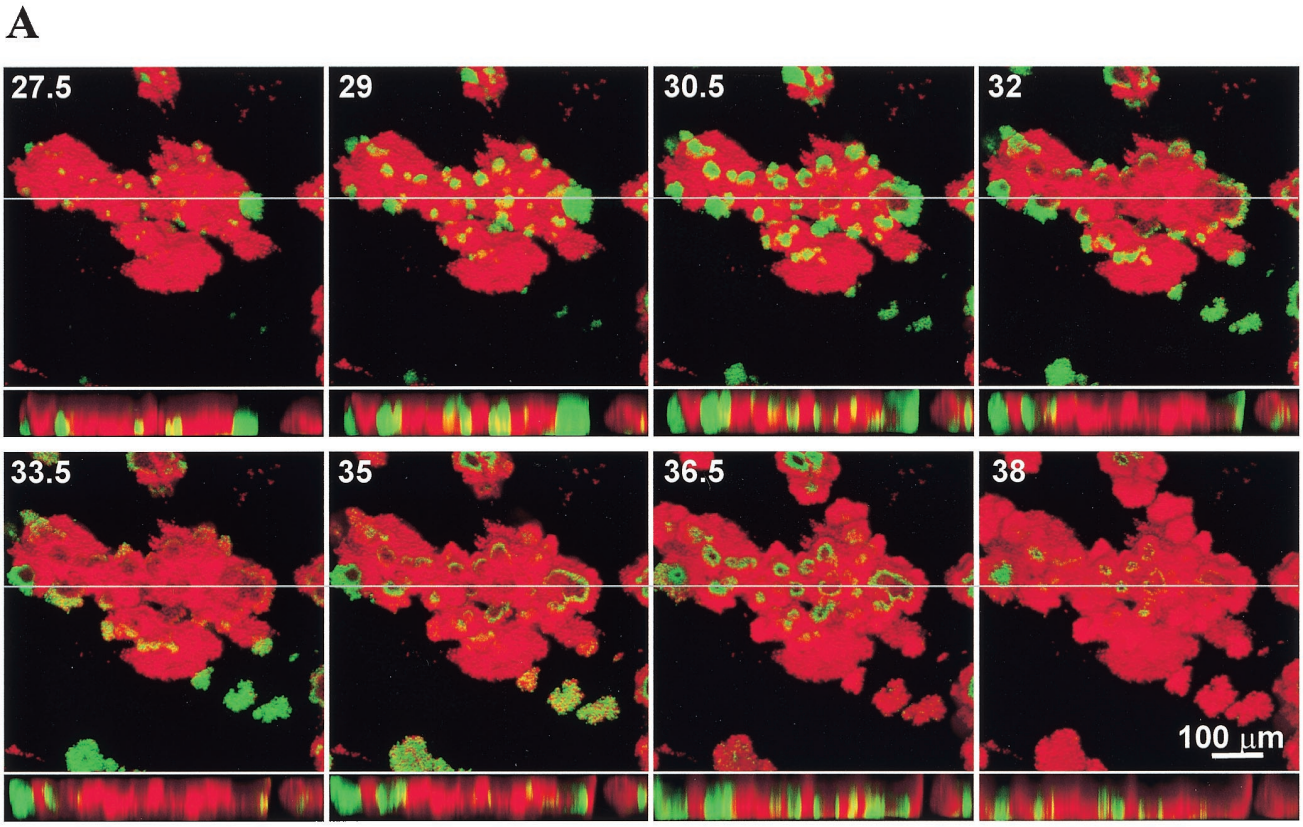

FIG. 5. Time lapse expression of the *agr* P3-*gfp* reporter in a flow cell biofilm of *S. aureus* MN8(pJY202). The images were acquired at 15-min intervals by using identical CSLM settings with a 20× objective lens. Green indicates those cells expressing the reporter, and the remainder of the biofilm appears red from treatment with propidium iodide. (A) Sequential images taken every 90 min are shown, with the number of hours postinoculation indicated. The larger images represent a compressed *z* series, where multiple *x-y* planes from top to bottom of the biofilm are combined. The smaller images represent *x-z* (side) views of the biofilm at the location indicated by the line. (B) Three-dimensional reconstruction of a *z* series taken ~36.5 h after inoculation in the experiment shown in panel A. Each side of a grid square represents 60 μm.

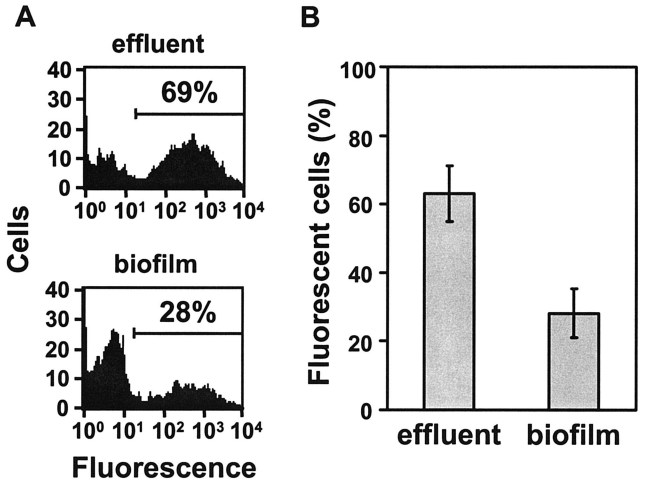

FIG. 6. Expression of the *agr* P3-*gfp* reporter in flow cell biofilms and effluents after 60 h. Effluents were collected for ~30 min from flow cells. Biofilms were then expelled from the same flow cells described in Materials and Methods. All collected cells were subsequently dispersed by ultrasonication and analyzed by flow cytometry for fluorescence (FL-1 channel). (A) Flow cytometry results from one representative flow cell biofilm and its effluent. The percentages represent the cells that fell within the range of fluorescence delineated by the marker. (B) Percentages of cells from quadruplicate flow cell biofilms and their effluents that were green fluorescent ± the standard deviation. The data are significant ($P < 0.001$; Student *t* test).

wide range of staphylococcal genes (13), it may well be that different genes or sets of genes regulated by the *agr* system influence *S. aureus* attachment and biofilm development under some growth conditions but not others. In some cases, *agr* expression likely affects the attachment of inoculum cells to a surface through its regulation of cell surface-associated adhesins. This could be the case in our static and spinning-disk reactor biofilms, as stationary-phase cells were diluted into fresh medium to inoculate these systems. In other cases, *agr* expression may also affect biofilm maturation, perhaps through its regulation of extracellular factors, such as δ-hemolysin (51). Due to the limitations of the static and spinning-disk reactor systems, we could not evaluate *agr* P3 reporter expression in situ using confocal microscopy to assess its effects on biofilm maturation.

In flow cell biofilms, we did not detect an influence of *agr* expression on biofilm development (Fig. 1C). Thus, one obvious question was whether *agr*-dependent promoters were even expressed in this type of system. We found that plasmid-borne quorum-controlled *agr* P3-*gfp* reporters were expressed in these biofilms (Fig. 3 to 5), as was a *sar* P1-*gfp* reporter (Fig. 7). Though fluorescence of cells containing the *sar* P1 reporter was observed earlier in microcolony growth than fluorescence of cells containing *agr* P3 reporters, both reporter types eventually showed similar oscillating patterns of expression. In any given area, we observed cycles with peaks in fluorescence followed by rapid losses of fluorescence. Furthermore, the oscillations in areas of close proximity often appeared to occur in synchrony, either simultaneously or sequentially (Fig. 4, 5, and 7). At any given time, there appeared to be clusters of cells expressing the fluorescent reporter surrounded by nonfluorescent cells (Fig. 3, 5, and 7).

How might the complex patterns of fluorescent reporter expression in the flow cell biofilms be explained? There are at least three possible explanations for loss of GFP fluorescence.

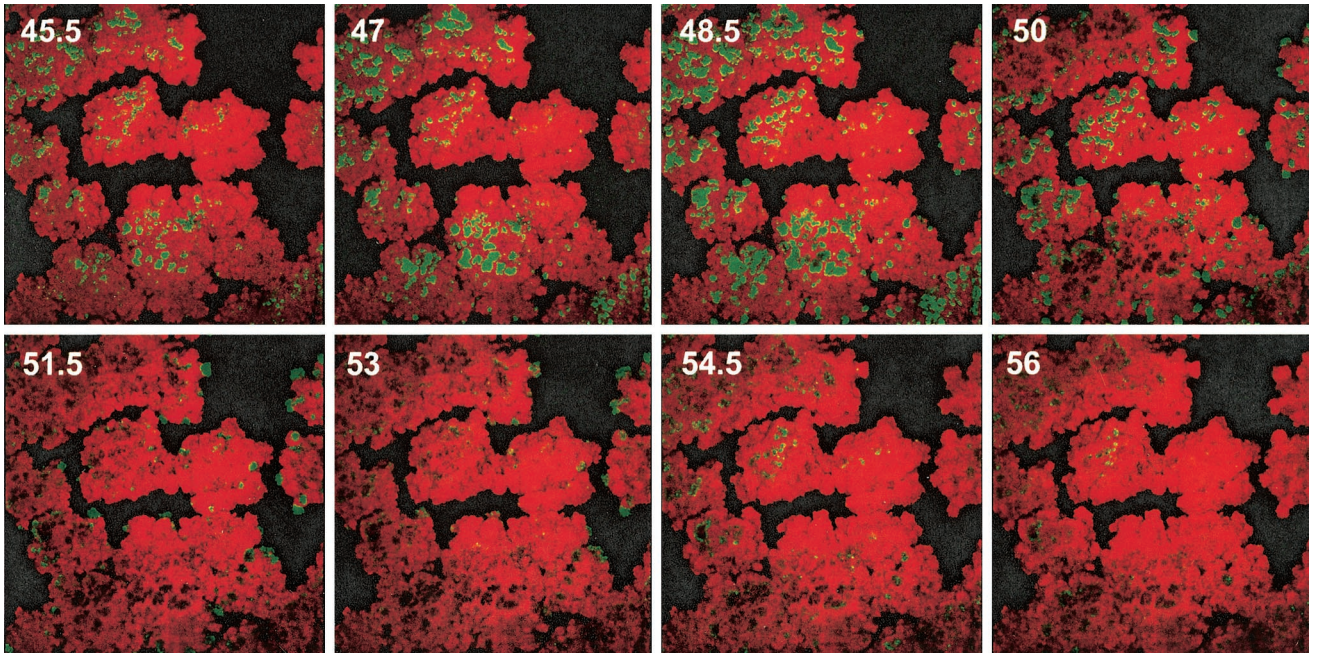

FIG. 7. Time lapse expression of the *sar* P1-*gfp* reporter in a flow cell biofilm of *S. aureus* MN8(pJY209). The images were acquired at 15-min intervals by using identical CSLM settings with a 20× objective lens. Green indicates those cells expressing the reporter, and the remainder of the biofilm appears red from treatment with propidium iodide. Sequential images taken every 90 min are shown, with the number of hours postinoculation indicated.

First, the GFP might be degraded, which seems unlikely considering that we have employed two versions of a GFP molecule with half-lives greater than 24 h (1, 47) with similar results. Second, cells may lyse or lose GFP through membrane disruption. We have observed a portion of the cell population, particularly in the peripheries of microcolonies, that appears to lose green fluorescence and then subsequently stains with propidium iodide (data not shown), suggesting loss of membrane integrity. These cells appear to remain part of the biofilm, together with the extracellular matrix. Third, loss of fluorescence might result from cell detachment from the biofilm. Often, cells expressing the *agr* P3-*gfp* reporter disappeared from the biofilm, leaving behind a void in propidium iodide-stained biofilms. This was followed by what appeared to be new growth of fluorescent cells in the void (Fig. 4, hours 13 to 17.5; Fig. 5A, hours 35 to 38). The fact that most of the biofilm appeared to remain intact and apparent voids were filled by new growth was consistent with our inability to detect any significant structural differences between biofilms formed by the wild type and the *agrD* mutant (Fig. 1C). Further evidence for fluorescent-cell detachment is our finding that the percentage of fluorescent cells in effluents from flow cells is significantly higher than the percentage of fluorescent cells within the flow cell biofilm (Fig. 6).

Our observations regarding oscillation of GFP fluorescence in flow cell biofilms, coupled with the fact that the oscillations in fluorescence were not unique to the expression of an *agr* reporter, suggest a broader model of gene expression in the biofilm that is closely related to both cell viability and detachment (Fig. 8). Only actively growing areas of the biofilm express the fluorescent reporters, and where conditions are appropriate within a sufficiently large cluster of actively growing cells, expression of quorum-controlled genes will be activated. Once cell clusters reach a sufficient size or age, most cells either detach or die. Additional growth then occurs in the voids left by detached cells. Thus, it is the cycle of cell growth, detachment, and regrowth that underlies the patterns of gene expression observed. Expression of surface-associated adhesins and *agr*-induced extracellular factors (51), localized shear forces, cell viability, and growth patterns may all contribute to the detachment of cells from the biofilm. Further investigation will be required to determine how these complex phenomena interact and contribute to the patterns of gene expression that we have observed.

A picture that emerges from the time course studies is that in most areas of a biofilm at most times, *agr*, and likely *agr*-dependent virulence genes, is not expressed. However, cells that do express *agr* appear to be released from the biofilm, cells that may also be expressing *agr*-dependent virulence factors. Our biofilm model is reminiscent of one previously proposed for *agr* expression by staphylococci in abscess infections (39), where crowding within the localized infection activates the *agr*-dependent quorum response and synthesis of extracellular factors, enabling the staphylococci to escape the abscess and spread to new sites. If this aspect of the biofilm model, that there is dispersion of virulent staphylococci, holds true, it will have important implications for the etiology of *S. aureus* biofilm infections.

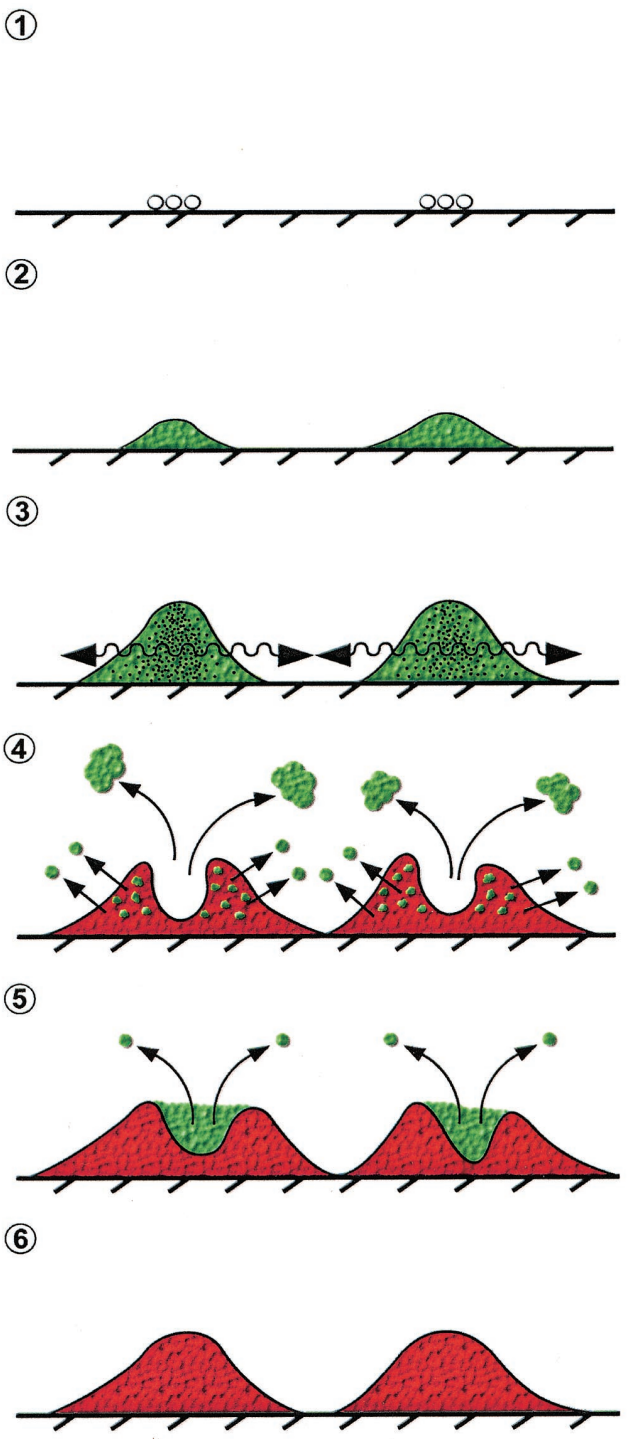

FIG. 8. Model of *agr* expression in *S. aureus* biofilms. After initial colonization by individual cells (step 1), microcolonies reach sufficient cell density for *agr*-dependent gene expression (step 2) and perhaps signaling between microcolonies (step 3, arrows). Portions of the biofilm detach through as-yet-unknown mechanisms (step 4), as either large aggregates or individual cells. Simultaneously, parts of the biofilm population become metabolically inactive and lose membrane integrity and green fluorescence. This is followed by new growth into the voids left by the detached cells (step 5), and the cycle is repeated. The microcolony finally reaches a relatively quiescent state where any growth is slow and *agr* expression is undetectable (step 6).

ACKNOWLEDGMENTS

This research was supported by a gift from the Procter and Gamble Company, Cincinnati, Ohio, and a grant from the W. M. Keck Foundation. J.M.Y. was supported by a U.S. Public Health Training Grant (T32-AI07511).

We acknowledge Patrick Schlievert for his provision of strains and general encouragement; Kimberly Lee, Pradeep Singh, Thomas Moninger, and the Central Microscopy Research Facility for materials and assistance with confocal microscopy; and Shirley Taylor and the Creative Media Group for figure illustrations. We thank Debra Murray, Timothy Yahr, and Catherine Davis for helpful discussions and critical reading of the manuscript.

REFERENCES

1. **Andersen, J. B., C. Sternberg, L. K. Poulsen, S. P. Bjorn, M. Givskov, and S. Molin.** 1998. New unstable variants of green fluorescent protein for studies of transient gene expression in bacteria. Appl. Environ. Microbiol. **64:**2240–2246.
2. **Beenken, K. E., J. S. Blevins, and M. S. Smeltzer.** 2003. Mutation of *sarA* in *Staphylococcus aureus* limits biofilm formation. Infect. Immun. **71:**4206–4211.
3. **Blevins, J. S., M. O. Elasri, S. D. Allmendinger, K. E. Beenken, R. A. Skinner, J. R. Thomas, and M. S. Smeltzer.** 2003. Role of *sarA* in the pathogenesis of *Staphylococcus aureus* musculoskeletal infection. Infect. Immun. **71:**516–523.
4. **Caiazza, N. C., and G. A. O'Toole.** 2003. Alpha-toxin is required for biofilm formation by *Staphylococcus aureus*. J. Bacteriol. **185:**3214–3217.
5. **Ceri, H., M. E. Olson, C. Stremick, R. R. Read, D. Morck, and A. Buret.** 1999. The Calgary Biofilm Device: new technology for rapid determination of antibiotic susceptibilities of bacterial biofilms. J. Clin. Microbiol. **37:**1771–1776.
6. **Cheung, A. L., M. G. Bayer, and J. H. Heinrichs.** 1997. *sar* genetic determinants necessary for transcription of RNAII and RNAIII in the *agr* locus of *Staphylococcus aureus*. J. Bacteriol. **179:**3963–3971.
7. **Cheung, A. L., K. J. Eberhardt, E. Chung, M. R. Yeaman, P. M. Sullam, M. Ramos, and A. S. Bayer.** 1994. Diminished virulence of a *sar*$^-$/*agr*$^-$ mutant of *Staphylococcus aureus* in the rabbit model of endocarditis. J. Clin. Investig. **94:**1815–1822.
8. **Cheung, A. L., C. C. Nast, and A. S. Bayer.** 1998. Selective activation of *sar* promoters with the use of green fluorescent protein transcriptional fusions as the detection system in the rabbit endocarditis model. Infect. Immun. **66:**5988–5993.
9. **Christensen, G. D., W. A. Simpson, J. J. Younger, L. M. Baddour, F. F. Barrett, D. M. Melton, and E. H. Beachey.** 1985. Adherence of coagulase-negative staphylococci to plastic tissue culture plates: a quantitative model for the adherence of staphylococci to medical devices. J. Clin. Microbiol. **22:**996–1006.
10. **Cormack, B. P., R. H. Valdivia, and S. Falkow.** 1996. FACS-optimized mutants of the green fluorescent protein (GFP). Gene **173:**33–38.
11. **Davies, D. G., M. R. Parsek, J. P. Pearson, B. H. Iglewski, J. W. Costerton, and E. P. Greenberg.** 1998. The involvement of cell-to-cell signals in the development of a bacterial biofilm. Science **280:**295–298.
12. **Donlan, R. M., and J. W. Costerton.** 2002. Biofilms: survival mechanisms of clinically relevant microorganisms. Clin. Microbiol. Rev. **15:**167–193.
13. **Dunman, P. M., E. Murphy, S. Haney, D. Palacios, G. Tucker-Kellogg, S. Wu, E. L. Brown, R. J. Zagursky, D. Shlaes, and S. J. Projan.** 2001. Transcription profiling-based identification of *Staphylococcus aureus* genes regulated by the *agr* and/or *sarA* loci. J. Bacteriol. **183:**7341–7353.
14. **Freed, R. C., M. L. Evenson, R. F. Reiser, and M. S. Bergdoll.** 1982. Enzyme-linked immunosorbent assay for detection of staphylococcal enterotoxins in foods. Appl. Environ. Microbiol. **44:**1349–1355.
15. **Gillaspy, A., S. Hickmon, R. Skinner, J. Thomas, C. Nelson, and M. Smeltzer.** 1995. Role of the accessory gene regulator (*agr*) in pathogenesis of staphylococcal osteomyelitis. Infect. Immun. **63:**3373–3380.
16. **Goerke, C., S. Campana, M. G. Bayer, G. Doring, K. Botzenhart, and C. Wolz.** 2000. Direct quantitative transcript analysis of the *agr* regulon of *Staphylococcus aureus* during human infection in comparison to the expression profile in vitro. Infect. Immun. **68:**1304–1311.
17. **Goerke, C., U. Fluckiger, A. Steinhuber, W. Zimmerli, and C. Wolz.** 2001. Impact of the regulatory loci *agr*, *sarA* and *sae* of *Staphylococcus aureus* on the induction of alpha-toxin during device-related infection resolved by direct quantitative transcript analysis. Mol. Microbiol. **40:**1439–1447.
18. **Gotz, F.** 2002. *Staphylococcus* and biofilms. Mol. Microbiol. **43:**1367–1378.
19. **Gryczan, T. J., G. Grandi, J. Hahn, R. Grandi, and D. Dubnau.** 1980. Conformational alteration of mRNA structure and the posttranscriptional regulation of erythromycin-induced drug resistance. Nucleic Acids Res. **8:**6081–6097.
20. **Hentzer, M., G. M. Teitzel, G. J. Balzer, A. Heydorn, S. Molin, M. Givskov, and M. R. Parsek.** 2001. Alginate overproduction affects *Pseudomonas aeruginosa* biofilm structure and function. J. Bacteriol. **183:**5395–5401.
21. **Heydorn, A., B. Ersboll, J. Kato, M. Hentzer, M. R. Parsek, T. Tolker-Nielsen, M. Givskov, and S. Molin.** 2002. Statistical analysis of *Pseudomonas aeruginosa* biofilm development: impact of mutations in genes involved in twitching motility, cell-to-cell signaling, and stationary-phase sigma factor expression. Appl. Environ. Microbiol. **68:**2008–2017.
22. **Huber, B., K. Riedel, M. Hentzer, A. Heydorn, A. Gotschlich, M. Givskov, S. Molin, and L. Eberl.** 2001. The *cep* quorum-sensing system of *Burkholderia cepacia* H111 controls biofilm formation and swarming motility. Microbiology **147:**2517–2528.
23. **Huber, B., K. Riedel, M. Kothe, M. Givskov, S. Molin, and L. Eberl.** 2002. Genetic analysis of functions involved in the late stages of biofilm development in *Burkholderia cepacia* H111. Mol. Microbiol. **46:**411–426.
24. **Kreiswirth, B. N., S. Lofdahl, M. J. Betley, M. O'Reilly, P. M. Schlievert, M. S. Bergdoll, and R. P. Novick.** 1983. The toxic shock syndrome exotoxin structural gene is not detectably transmitted by a prophage. Nature **305:**709–712.
25. **Leid, J. G., M. E. Shirtliff, J. W. Costerton, and A. P. Stoodley.** 2002. Human leukocytes adhere to, penetrate, and respond to *Staphylococcus aureus* biofilms. Infect. Immun. **70:**6339–6345.
26. **Li, Y. H., N. Tang, M. B. Aspiras, P. C. Y. Lau, J. H. Lee, R. P. Ellen, and D. G. Cvitkovitch.** 2002. A quorum-sensing signaling system essential for genetic competence in *Streptococcus mutans* is involved in biofilm formation. J. Bacteriol. **184:**2699–2708.
27. **Lynch, M. J., S. Swift, D. F. Kirke, C. W. Keevil, C. E. Dodd, and P. Williams.** 2002. The regulation of biofilm development by quorum sensing in *Aeromonas hydrophila*. Environ. Microbiol. **4:**18–28.
28. **Mandell, G. L., J. E. Bennett, and R. Dolin (ed.).** 1995. Mandell, Douglas and Bennett's Principles and practice of infectious diseases, 4th ed. Churchill Livingstone, New York, N.Y.
29. **Manna, A. C., M. G. Bayer, and A. L. Cheung.** 1998. Transcriptional analysis of different promoters in the *sar* locus in *Staphylococcus aureus*. J. Bacteriol. **180:**3828–3836.
30. **Mayberry-Carson, K. J., B. Tober-Meyer, J. K. Smith, D. W. Lambe, Jr., and J. W. Costerton.** 1984. Bacterial adherence and glycocalyx formation in osteomyelitis experimentally induced with *Staphylococcus aureus*. Infect. Immun. **43:**825–833.
31. **Merritt, J., F. Qi, S. D. Goodman, M. H. Anderson, and W. Shi.** 2003. Mutation of *luxS* affects biofilm formation in *Streptococcus mutans*. Infect. Immun. **71:**1972–1979.
32. **Morfeldt, E., K. Tegmark, and S. Arvidson.** 1996. Transcriptional control of the *agr*-dependent virulence gene regulator, RNAIII, in *Staphylococcus aureus*. Mol. Microbiol. **21:**1227–1237.
33. **Murray, D. L., C. A. Earhart, D. T. Mitchell, D. H. Ohlendorf, R. P. Novick, and P. M. Schlievert.** 1996. Localization of biologically important regions on toxic shock syndrome toxin 1. Infect. Immun. **64:**371–374.
34. **NCCLS.** 2000. Methods for dilution antimicrobial susceptibility tests for bacteria that grow aerobically; approved standard M7-A5, 5th ed., vol. 20. NCCLS, Wayne, Pa.
35. **Novick, R. P.** 2000. Pathogenicity factors and their regulation, p. 392–407. *In* V. A. Fischetti, R. P. Novick, J. J. Ferretti, D. A. Portnoy, and J. I. Rood (ed.), Gram-positive pathogens. ASM Press, Washington, D.C.
36. **Oie, S., Y. Huang, A. Kamiya, H. Konishi, and T. Nakazawa.** 1996. Efficacy of disinfectants against biofilm cells of methicillin-resistant *Staphylococcus aureus*. Microbios **85:**223–230.
37. **Parsek, M. R., and E. P. Greenberg.** 1999. Quorum sensing signals in development of *Pseudomonas aeruginosa* biofilms. Methods Enzymol. **310:**43–55.
38. **Pratten, J., S. J. Foster, P. F. Chan, M. Wilson, and S. P. Nair.** 2001. *Staphylococcus aureus* accessory regulators: expression within biofilms and effect on adhesion. Microbes Infect. **3:**633–637.
39. **Projan, S. J., and R. P. Novick.** 1997. The molecular basis of pathogenicity, p. 55–81. *In* K. B. Crossley and G. L. Archer (ed.), The staphylococci in human disease. Churchill Livingstone Inc., New York, N.Y.
40. **Schenk, S., and R. A. Laddaga.** 1992. Improved method for electroporation of *Staphylococcus aureus*. FEMS Microbiol. Lett. **73:**133–138.
41. **Schlievert, P. M., and D. A. Blomster.** 1983. Production of staphylococcal pyrogenic exotoxin type C: influence of physical and chemical factors. J. Infect. Dis. **147:**236–242.
42. **Shenkman, B., D. Varon, I. Tamarin, R. Dardik, M. Peisachov, N. Savion, and E. Rubinstein.** 2002. Role of *agr* (RNAIII) in *Staphylococcus aureus* adherence to fibrinogen, fibronectin, platelets and endothelial cells under static and flow conditions. J. Med. Microbiol. **51:**747–754.
43. **Shiau, A. L., and C. L. Wu.** 1998. The inhibitory effect of *Staphylococcus epidermidis* slime on the phagocytosis of murine peritoneal macrophages is interferon-independent. Microbiol. Immunol. **42:**33–40.
44. **Shirtliff, M. E., J. T. Mader, and A. K. Camper.** 2002. Molecular interactions in biofilms. Chem. Biol. **9:**859–871.
45. **Smith, K., and P. Youngman.** 1992. Use of a new integrational vector to investigate compartment-specific expression of the *Bacillus subtilis spoIIM* gene. Biochimie **74:**705–711.
46. **Steidle, A., M. Allesen-Holm, K. Riedel, G. Berg, M. Givskov, S. Molin, and L. Eberl.** 2002. Identification and characterization of an *N*-acylhomoserine lactone-dependent quorum-sensing system in *Pseudomonas putida* strain IsoF. Appl. Environ. Microbiol. **68:**6371–6382.

47. **Tombolini, R., A. Unge, M. E. Davey, F. J. D. Bruijn, and J. K. Jansson.** 1997. Flow cytometric and microscopic analysis of GFP-tagged *Pseudomonas fluorescens* bacteria. FEMS Microbiol. Ecol. **22:**17–28.
48. **Valle, J., A. Toledo-Arana, C. Berasain, J. M. Ghigo, B. Amorena, J. R. Penades, and I. Lasa.** 2003. SarA and not σ^B is essential for biofilm development by *Staphylococcus aureus*. Mol. Microbiol. **48:**1075–1087.
49. **Vance, R. E., J. Zhu, and J. J. Mekalanos.** 2003. A constitutively active variant of the quorum-sensing regulator LuxO affects protease production and biofilm formation in *Vibrio cholerae*. Infect. Immun. **71:**2571–2576.
50. **van Wamel, W., Y. Q. Xiong, A. Bayer, M. Yeaman, C. Nast, and A. Cheung.** 2002. Regulation of *Staphylococcus aureus* type 5 capsular polysaccharides by *agr* and *sarA* in vitro and in an experimental endocarditis model. Microb. Pathog. **33:**73–79.
51. **Vuong, C., H. L. Saenz, F. Gotz, and M. Otto.** 2000. Impact of the *agr* quorum-sensing system on adherence to polystyrene in *Staphylococcus aureus*. J. Infect. Dis. **182:**1688–1693.
52. **Weisblum, B., M. Y. Graham, T. Gryczan, and D. Dubnau.** 1979. Plasmid copy number control: isolation and characterization of high-copy-number mutants of plasmid pE194. J. Bacteriol. **137:**635–643.
53. **Xiong, Y. Q., W. Van Wamel, C. C. Nast, M. R. Yeaman, A. L. Cheung, and A. S. Bayer.** 2002. Activation and transcriptional interaction between *agr* RNAII and RNAIII in *Staphylococcus aureus* in vitro and in an experimental endocarditis model. J. Infect. Dis. **186:**668–677.
54. **Yarwood, J. M., J. K. McCormick, M. L. Paustian, V. Kapur, and P. M. Schlievert.** 2002. Repression of the *Staphylococcus aureus* accessory gene regulator in serum and in vivo. J. Bacteriol. **184:**1095–1101.
55. **Yarwood, J. M., and P. M. Schlievert.** 2000. Oxygen and carbon dioxide regulation of toxic shock syndrome toxin 1 production by *Staphylococcus aureus* MN8. J. Clin. Microbiol. **38:**1797–1803.